Hydrogen collision model: Quantitative description of metastability in amorphous silicon

Howard M. Branz
National Renewable Energy Laboratory, Golden, Colorado 80401
(Received 16 March 1998; revised manuscript received 2 October 1998)

The hydrogen collision model of light-induced metastability in hydrogenated amorphous silicon is described in detail. Recombination of photogenerated carriers excites mobile H from Si-H bonds, leaving threefold-coordinated Si dangling-bond defects. When two mobile H atoms collide and associate in a metastable two-H complex, the two dangling bonds from which H was emitted also become metastable. The proposed microscopic mechanism is consistent with electron-spin-resonance experiments. Comprehensive rate equations for the dangling-bond and mobile-H densities are presented; these equations include light-induced creation and annealing. Important regimes are solved analytically and numerically. The model provides explanations for both the $t^{1/3}$ time dependence of the rise of defect density during continuous illumination and the $t^{1/2}$ time-dependence during intense laser-pulse illumination. Other consequences and predictions of the H collision model are described. [S0163-1829(99)04308-8]

I. INTRODUCTION

Semiconducting hydrogenated amorphous silicon (a-Si:H) thin films can be grown with fewer than 10^{15}-cm^{-3} neutral threefold-coordinated Si dangling-bond (DB) defects. However, the introduction of excess carriers through moderate illumination or electronic injection increases the density of DB's to nearly $10^{17}\,cm^{-3}$, even in the most degradation-resistant materials.[1–5] These excess carrier-induced DB's are metastable; they are annealed out in a few hours at about 150 °C. However, their rapid formation sharply limits application of a-Si:H as an inexpensive material for photovoltaic and electronic applications. The source of the carrier-induced metastability has been elusive; since its discovery by Staebler and Wronski[6] (SW) in 1976, dozens of models have been published, but no previous model is satisfactory.[7,8]

Recently, I published a preliminary report[9] of a ''hydrogen collision'' model that explains the main experimental observations of the SW effect, both quantitatively and qualitatively. Recombination-induced emission of H from Si-H bonds creates both mobile H in transport and DB's. The newly created DB's become metastable when the mobile H collide to form metastable complexes containing two Si-H bonds. The term ''collision'' is not intended to connote direct contact between the two H atoms; rather, it describes the association of two mobile H into a metastable paired configuration. In this paper, I develop the model and its consequences, in detail.

Section II presents a microscopic description of the H collision model and summarizes its advantages compared to previous models. Section III introduces the differential equations describing light-induced defect creation and annealing. Section IV presents several asymptotic closed-form solutions of the model, including a model of high-intensity pulsed-laser degradation. Section V shows numerical solutions that support the asymptotic solutions. Section VI treats thermal equilibrium and dark thermal equilibration of DB's. The Appendix examines the recombination-induced emission of mobile H. This exploration of the H collision model will permit researchers to devise experimental tests of model predictions.

II. MICROSCOPIC MODELS

A. H collision model

Hydrogenated amorphous silicon contains from 1- to 25-at. % hydrogen. Most device quality a-Si:H contains about 10 at. % of H; almost every H forms a Si-H bond with a Si that is bonded to only three other Si atoms. In the H collision model[9] of the SW effect, DB's are created when recombination of light-induced carriers stimulates emission of mobile H from Si-H bonds according to:

$$\text{Si-H} \rightarrow \text{DB} + \text{Si-H/DB}. \tag{1}$$

The mobile H, notated here by Si-H/DB, is usually modeled as a mobile Si-H-Si bond-centered H configuration. However, it is useful to visualize mobile H as a mobile Si-H bond accompanied by a mobile DB. The tight-binding molecular-dynamics simulations of Biswas *et al.*[10] support this view; they showed that mobile H's break Si-Si bonds and form Si-H bonds as they hop between Si-Si sites. Each broken Si-Si bond reforms as the mobile H hops away. Mobile H is weakly bound compared to H in normal Si-H bonds; the mobile H diffuses rapidly through a-Si:H.[11]

Mobile H retraps to Si-H through one of two mechanisms. Normal retrapping to an immobile DB is given by

$$\text{Si-H/DB} + \text{DB} \rightarrow \text{Si-H}, \tag{2}$$

the inverse process to Eq. (1). This trapping is usually envisioned simply as H jumping to the ordinary DB. However, it can be understood instead as formation of a bond between the mobile DB and the immobile DB on the left of Eq. (2). In this case, the H remains bonded to a single Si atom as it is immobilized by the process of Eq. (2). No net DB's are created if H reconfigures only through the cyclical processes of Eqs. (1) and (2)—this is the ''normal'' creation and retrapping of mobile H.

A second retrapping process

$$\text{Si-H/DB} + \text{Si-H/DB} \rightarrow M(\text{Si-H})_2 \tag{3}$$

 ©1999 The American Physical Society

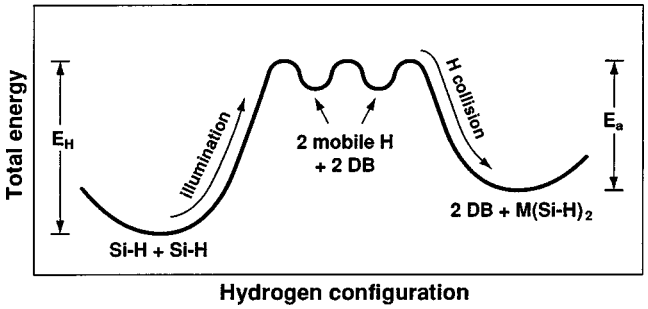

FIG. 1. Configuration-coordinate diagram of the Staebler-Wronski DB creation reaction of Eq. (4). Leftmost and rightmost wells are the stable and metastable states, respectively. Only two of many degenerate intermediate states with mobile H are represented by the central wells. Hydrogen diffusion (E_H) and metastability annealing (E_a) energies are indicated.

is far less frequent than normal retrapping, but is important as a key step of SW defect creation. Equation (3) represents a collision of two mobile H atoms that associate into a metastable complex, $M(\text{Si-H})_2$, containing a pair of Si-H bonds in close proximity. This reaction begins when the two mobile DB's (traveling with mobile H) come close enough together to form a Si-Si bond. The two mobile H's are then immobilized and form $M(\text{Si-H})_2$. The reaction annihilates two mobile DB's and forms no DB's, consistent with bond-counting constraints. Because energetic Si-H/DB's are annihilated, the reaction of Eq. (3) is strongly exothermic.[12] Combining Eqs. (1) and (3), the net reaction leaves DB defects at the sites of the original H excitation according to

$$2\text{Si-H}\rightarrow 2\text{DB}+2\text{Si-H/DB}\rightarrow 2\text{DB}+M(\text{Si-H})_2. \qquad (4)$$

The created SW DB's appear on the rightmost side of Eq. (4). Figure 1 shows a configuration-coordinate diagram of the Eq. (4) reaction.

The first step of light-induced or thermal annealing of the SW effect is the back reaction of Eq. (3). Emission of one mobile H from $M(\text{Si-H})_2$ leaves a DB and a Si-H bond in close proximity to one another. By pairing with the DB, this second H soon becomes mobile through a low-barrier process. Thus $M(\text{Si-H})_2$ is a negative-U hydrogen pair of the class described by Zafar and Schiff,[13] although it may not take the microscopic form they proposed. Under most conditions, the normal retrapping of mobile H to DB's [Eq. (2)] will dominate the retrapping of any H emitted from $M(\text{Si-H})_2$. This second step completes the SW annealing.

Figure 2 depicts the SW reaction of Eq. (4). The distances that the two mobile H's travel before collision are actually much greater than those illustrated. Inside the dashed oval of Fig. 2 is one of many conceivable structures of $M(\text{Si-H})_2$. This particular structure is an asymmetric configuration of the two H atoms. Two other possibilities for the proposed $M(\text{Si-H})_2$ center are sketched in Fig. 3. Figure 3(a) illustrates the suggestion of Biswas and Pan[12] that $M(\text{Si-H})_2$ may be the H_2^* center previously proposed for both crystalline[14] and amorphous Si.[15] Figure 3(b) illustrates a configuration of the doubly hydrogenated Si-Si bond (Si-H H-Si) proposed as a negative correlation energy two-H center by Zafar and Schiff.[13] None of the candidate $M(\text{Si-H})_2$ centers contain DB's.

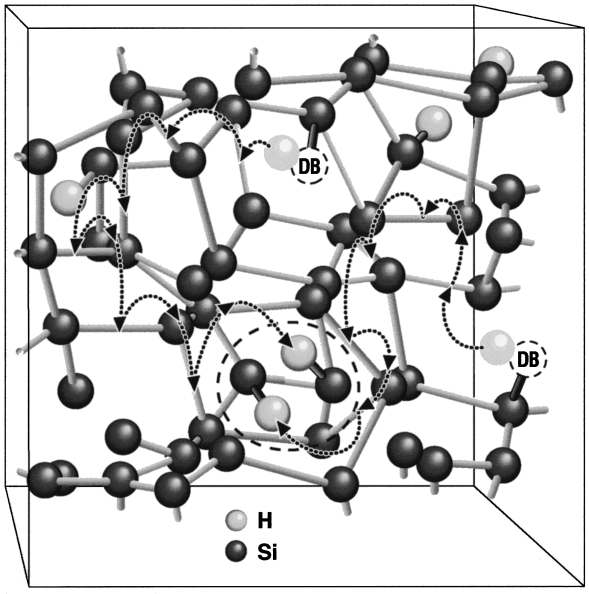

FIG. 2. Schematic diagram of the Staebler-Wronski DB creation reaction of Eq. (4). The dotted mobile H diffusion paths are shorter than the actual distances normally traveled. One alternative for the metastable complex $M(\text{Si-H})_2$ is indicated inside the dashed oval.

The most important constraint upon $M(\text{Si-H})_2$ is supplied by the SW annealing data. While thermal emission of H from Si-H into transport requires about $E_H = 1.5\,\text{eV}$,[11] annealing of the SW requires only about $E_a = 1.1\,\text{eV}$.[16] Figure 1 indicates E_H and E_a, the energies required to surmount the barrier to H transport from normal Si-H and from $M(\text{Si-H})_2$, respectively. Biswas and Pan[12] show that either the H_2^* or a configuration in which the two H's face away from one another (H-Si Si-H), can have total energies per Si-H about 0.37 eV higher than isolated Si-H, consistent with the constraint that E_H-$E_a \sim 0.4\,\text{eV}$. However, they found the configuration of Fig. 3(b) (Si-H H-Si), was too energetic to identify with $M(\text{Si-H})_2$.

B. Comparison with previous models

A great many microscopic models of the SW effect have been proposed during the 20 years since its discovery. These

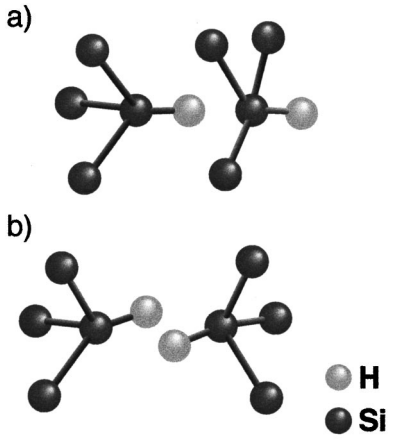

FIG. 3. Schematic diagram of two alternatives to the $M(\text{Si-H})_2$ complex illustrated in Fig. 2. They are (a) the H_2^* analog center proposed by Biswas and Pan (Ref. 12) and (b) a doubly hydrogenated Si-Si bond.

are reviewed in detail elsewhere,[7,8,17,18] and are discussed here only in general terms. I describe previous models to provide a context for the H collision model and to highlight the inability of previous models to account for well-established experimental observations. I also contrast the present model with several closely related models from which elements of the present model are taken.

The entire class of impurity-related microscopic models in which an impurity atom is associated with each SW DB is eliminated from serious consideration by the recent work of Kamei *et al.*[19] By carefully controlling and measuring the purity of their *a*-Si:H samples, they observed SW defect densities orders of magnitude greater than the densities of C, N, and O. Other impurities such as P and B are not present in many deposition chambers, but the SW effect is quite universal. One can conclude that the SW effect is *intrinsic* to the network of Si and H atoms.

Two main Si-only models of the SW effect have been proposed. First, various authors discussed the possibility that the breaking of weak Si-Si bonds under illumination produces the DB defects.[20,21] However, the electron-spin-resonance (ESR) spectrum of the SW DB's shows no signs of the exchange narrowing that a neighboring pair of DB's would produce.[22] Also, it is difficult to understand why the broken bond would not simply reform. For these reasons, the bond-breaking model is thought to require a H hop to stabilize the SW DB's.[23] However, this H stabilization of the broken Si-Si bond appears to be excluded by ESR hyperfine studies showing that SW DB's are not spatially correlated with H atoms.[8,24] In fact, this ESR data would exclude the entire class of models involving local motion of H, as first proposed by Staebler and Wronski.[25]

Adler[26] proposed a second Si-only model, in which pre-existing charged DB defects capture photogenerated charge and reconfigure into metastable neutral DB's. However, measured charged DB densities[27] appear to be too low to support this model, and the measured time dependence of the metastable DB density, $N_{\rm db}(t) \propto t^{1/3}$,[23] seems to be incompatible with a one-carrier creation mechanism.[21] Also, recent molecular-dynamics studies of DB relaxation in response to charge capture show no indications of the energy barriers that would be required to form metastable DB's in this model.[28]

With impurity, Si-only, and local-H models of the SW effect rendered implausible by recent experimental results, the most promising class of models involve long-range diffusion of H. In nearly all of these models, a DB forms where light-induced carriers stimulate emission of H from Si-H bonds, as in Eq. (1) of the H collision model. The mobile H then diffuses to another location where it retraps. The H emission [Eq. (1)] leaves an isolated DB uncorrelated with H, consistent with the ESR data.[8,24] A connection between light-induced H emission and metastability is qualitatively supported by studies of light-induced H diffusion.[29,30]

Several other long-range H diffusion models preceded the H collision model. Carlson[31] suggested that the diffusing H atom finds its way to the internal surface of a microvoid, and is metastable there after some reconstruction. Jackson and Zhang[32] proposed that H is emitted from a Si-H bond of a H_2^* complex and traps at a strained Si-Si bond to form Si-H and a DB. (These authors also considered impurity trapping sites, but this is excluded by the experiments of Kamei *et al.*,[19] described above.) Santos, Johnson and Street[29] proposed emission from Si-H followed by retrapping at a Si-Si bond to form Si-H and a second DB.

All of these long-range diffusion models suffer the same difficulty: the SW DB at the site of H retrapping is in close proximity to H. Topological (bond-counting) considerations require that a DB is created whenever a single mobile H is trapped into a region comprised only of fourfold-coordinated Si atoms and H bonded as Si-H. This DB should show a H hyperfine signature that is not found by the ESR studies.[8,24] The H collision model of Sec. II A overcomes the shortcomings of these models by proposing a spin-inactive final state for the two mobile H's that were released from Si-H.

Godet and Roca *i* Cabarrocas[33] (GR) proposed a distinct long-range H diffusion model of metastability. The first step of this SW model is light-induced emission of H from a pre-existing doubly-hydrogenated Si-Si bond:

$$\text{(Si-H H-Si)} \rightarrow \text{Si-Si} + 2\text{Si-H/DB}. \tag{5}$$

I have used my notation for the mobile H atoms in Eq. (5). In the GR model, SW DB's are created when mobile H atoms retrap, according to

$$\text{Si-H/DB} + \text{Si-H} \rightarrow \text{DB} + \text{Si-H H-Si}. \tag{6}$$

Light-induced annealing occurs when the mobile H atoms are retrapped according to the competing retrapping process of Eq. (2).

There are two problems with the GR model.[33] First, Eq. (6) implies that all SW-created DB's are in close proximity to H atoms. Again, this contradicts the ESR data.[8,24] Second, the SW capture process for the mobile H should be exothermic so it can (1) compete with the normal capture to the DB [Eq. (2)], and (2) produce a metastable center. The SW reaction of Eq. (6) conserves the total density of DB's and must therefore be nearly isoenergetic. The reaction may be even weakly endothermic if the mobile DB has lower total energy than the immobile DB. In contrast, SW retrapping in the H collision model, as given by Eq. (3), annihilates two DB's and is obviously exothermic. Therefore, the H's in $M(\text{Si-H})_2$ are deeply bound, and SW DB's can be metastable in the H collision model.

Stutzmann, Jackson, and Tsai[16,23] (SJT) based a model of defect creation kinetics upon the hypothesis that SW DB's are created by direct electron-hole pair recombination, but are not created by DB-mediated recombination. This hypothesis and the resulting creation kinetics need not be linked to any particular atomic model of the metastability. SJT derived the widely observed $N_{\rm db}(t) \propto G^{2/3} t^{1/3}$ kinetics[23] of SW DB creation from the competition between the direct and DB-mediated electron-hole pair recombination mechanisms. However, several recent experiments are incompatible with the proposed model. Stradins and Fritzsche[34] showed that $N_{\rm db}(t) \propto t^{1/3}$ kinetics are observed down to a temperature of 4.2 K at which DB's have little influence upon photocarrier concentrations.[35] In the SJT model, $t^{1/3}$ kinetics are a consequence of dominant DB-mediated recombination. Therefore, Fritzsche[7] argued that the SJT creation mechanism is not viable. Laser-pulse creation experiments provide further evi-

dence that the SJT mechanism is invalid,[36] an argument that is reviewed in detail in Sec. IV F 1.

The H collision model provides an alternative explanation of the $N_{db}(t) \propto G^{2/3} t^{1/3}$ kinetics of SW DB creation near room temperature (see Sec. IV A). In the H collision model, $N_{db}(t) \propto t^{1/3}$ remains valid at 4.2 K, under the assumption that mobile H diffusion can be driven by photocarriers (see Sec. IV E and Ref. 9). Finally, the H collision model accounts naturally for the laser-pulse experiments (see Sec. IV F).

III. RATE EQUATIONS

In this section, I propose rate equations that govern the kinetics of the H collision model described in Sec. II A. I apply the simple ansatz that the emission rate of mobile H from Si-H bonds [Eq. (1)] is proportional to G. The emission rate of mobile H is then $R_m = k_H N_H G$, where N_H is the immobile Si-H density, G is the generation rate of electron-hole pairs, and k_H is a proportionality constant (in cm^3). This form is suggested by light-induced D tracer diffusion experiments at 250 °C,[29] and should be taken as a zeroth-order approximation to more complicated physics of recombination-induced H emission. In the Appendix, I discuss this physics and solve the H collision rate equations using a more general form for R_m.

I begin with the assumption that N_H is constant because the mobile H and $M(\text{Si-H})_2$ densities are negligible at all times compared to the density of Si-H bonds contributing to reaction (1). The trapping rate of mobile H to ordinary DB's [Eq. (2)] is $k_{db} N_m N_{db}$, and the collision rate of mobile H [Eq. (3)] is $2k_c N_m^2$. The factor of 2 arises because two H's are lost in each H collision.[37] Here N_{db} is the dangling-bond density, N_m is the mobile H density, and k_{db} and k_c are rate constants (in $cm^3\,s^{-1}$). Because the retrapping processes of Eqs. (2) and (3) are similar, k_{db} and k_c may be nearly equal. I first assume that the light-induced emission of H from $M(\text{Si-H})_2$ [the reverse of Eq. (3)] is negligible. Then the coupled creation-only rate equations for N_m, N_{db}, and N_{HH}, the density of $M(\text{Si-H})_2$, are

$$dN_m/dt = k_H N_H G - k_{db} N_m N_{db} - 2k_c N_m^2, \tag{7a}$$

$$dN_{db}/dt = k_H N_H G - k_{db} N_m N_{db}, \tag{7b}$$

and

$$dN_{HH}/dt = k_c N_m^2. \tag{7c}$$

To derive rate equations including light-induced annealing, I assume the emission of H from $M(\text{Si-H})_2$ [the reverse of Eq. (3)] is also proportional to G, and define the emission proportionality constant, k_{HH}, to be analogous to k_H. The product Gk_{HH} is then defined as the rate of emission of a particular H from $M(\text{Si-H})_2$—this rate describes only the first H emitted. I assume that the second H is immediately mobile, due to its proximity to the remaining DB. This emission of the second mobile H atom completes the annealing of a $M(\text{Si-H})_2$. The emission rate of mobile H from $M(\text{Si-H})_2$ is therefore $4k_{HH} N_{HH} G$, and the annealing rate of $M(\text{Si-H})_2$ is $2k_{HH} N_{HH} G$, because there are two different H's that can be the first emitted. Inclusion of light-induced annealing augments Eqs. (7a) and (7c) with a new term, and leaves Eq. (7b) unchanged, to yield

$$dN_m/dt = k_H N_H G - k_{db} N_m N_{db} - 2k_c N_m^2 + 4k_{HH} N_{HH} G, \tag{8a}$$

$$dN_{db}/dt = k_H N_H G - k_{db} N_m N_{db}, \tag{8b}$$

and

$$dN_{HH}/dt = -2k_{HH} N_{HH} G + k_c N_m^2. \tag{8c}$$

Experiments suggest that thermal annealing terms are important during illumination only under certain conditions (e.g., a temperature above 100 °C, a low light level, and a high defect density). Thermal emission of H from $M(\text{Si-H})_2$ adds additional terms to Eqs. (8a) and (8c), respectively, as described in Sec. VI B 1.

I have assumed, above, that the immobile isolated Si-H density, N_H, is constant. For completeness, I relax this assumption and augment Eqs. (7) and (8) with

$$dN_H/dt = -k_H N_H G + k_{db} N_m N_{db}, \tag{9}$$

an equation that could become important *only* in cases in which N_H is significantly reduced through creation of other H-containing species, i.e., N_{HH} or N_m become very high.

The rate equations given by Eqs. (7), (8) and (9) apply only when mobile H diffusion is driven thermally. Their dependence upon G is altered if photogenerated electron-hole pairs drive mobile H diffusion, as discussed in Sec. IV E.

IV. ASYMPTOTIC SOLUTIONS AND MODEL CONSEQUENCES

A. $G^{2/3}t^{1/3}$ creation kinetics

Equations (7) are a system of coupled nonlinear differential equations that exhibit a variety of solutions in different regimes. In this section, asymptotic solutions for long-time continuous illumination are obtained. The approximations of this section are valid over a wide range of realistic initial conditions and parameters. The asymptotic solutions are confirmed by computer numerical solution in Sec. V B. The transient behavior is complex, and is treated in more detail in Sec. IV B below.

Each H emission from Si-H leaves a DB [Eq. (1)], so $N_{db} > N_m$ at all times. In this section, I assume a slightly more stringent condition of low mobile H density,

$$N_m \ll N_{db}, \tag{10}$$

that is met under most experimental conditions.

Two different timescales are normally important in the SW creation solutions of Eqs. (7). N_m reaches quasiequilibrium rapidly with N_{db}, through mobile H emission from Si-H and retrapping to DB's [Eqs. (1) and (2)]. Creation of DB's by mobile H collision [Eq. (3)] is a much slower process. The quasiequilibrium reached between N_m and N_{db} implies that N_{db}/dt and dN_m/dt both fall nearly to zero after an initial transient in both quantities. Setting $dN_{db}/dt = 0$ in Eq. (7b) yields the the density of mobile H in quasiequilibrium with N_{db},

$$N_m=(k_{\rm H}N_{\rm H}G)/(k_{\rm db}N_{\rm db}). \tag{11}$$

Equation (11) can also be obtained by setting $dN_m/dt=0$ in Eq. (7a) in the low mobile H limit [Eq. (10)].

Eventually, $N_{\rm db}$ begins to rise through H collisions [Eq. (4)], while N_m falls in quasiequilibrium with $N_{\rm db}$ [Eq. (11)]. The quasiequilibrium condition of Eq. (11) implies that the product $N_mN_{\rm db}$ is constant and $d(N_mN_{\rm db})/dt=0$. Expanding this derivative, $N_m|dN_{\rm db}/dt|=N_{\rm db}|dN_m/dt|$. Since $N_m \ll N_{\rm db}$ [Eq. (10)], $|dN_m/dt| \ll |dN_{\rm db}/dt|$. Subtracting Eq. (7a) from Eq. (7b), and neglecting dN_m/dt with respect to $dN_{\rm db}/dt$, implies

$$dN_{\rm db}/dt=2k_cN_m^2 \tag{12}$$

at long times. Inspection of Eqs. (7c) and (12) shows $dN_{\rm db}/dt=2dN_{\rm HH}/dt$. As expected, the the long-time increase in DB density results from creation of $M(\text{Si-H})_2$ centers [Eq. (4)].

Substituting Eq. (11) into Eq. (12) yields

$$dN_{\rm db}/dt=C_{\rm sw}G^2/N_{\rm db}^2, \tag{13a}$$

with

$$C_{\rm sw}=\frac{2k_ck_{\rm H}^2N_{\rm H}^2}{k_{\rm db}^2}. \tag{13b}$$

In the limit $N_{\rm db}(t) \geqslant 2N_{\rm db}(0)$, the long-time solution of Eq. (13a) is[23]

$$N_{\rm db}(t)=(3C_{\rm sw})^{1/3}G^{2/3}t^{1/3}. \tag{14}$$

Substituting Eq. (14) into Eq. (11) gives the long-time decay of the mobile H density due to the rise of $N_{\rm db}$:

$$N_m(t)=\frac{k_{\rm H}N_{\rm H}}{k_{\rm db}}\left(\frac{G}{3C_{\rm sw}}\right)^{1/3}t^{-1/3}. \tag{15}$$

Equation (14) gives the well-documented $G^{2/3}t^{1/3}$ creation kinetics first observed in Ref. 23. SJT derived Eq. (13a) from different physics, and obtained a completely different expression than Eq. (13b) for the Staebler-Wronski coefficient $C_{\rm sw}$. They obtained Eqs. (13a) and (14) by assuming SW DB formation through bimolecular recombination of electrons and holes with densities proportional to $G/N_{\rm db}$. However, experiments show that this form for the carrier densities is less general than the $t^{1/3}$ kinetics of Eq. (14), and that there are other problems with the recombination model,[7,34] as reviewed in Sec. II B.

The H collision model yields $G^{2/3}t^{1/3}$ kinetics because SW DB's are created through bimolecular recombination of mobile H that has a density proportional to $G/N_{\rm db}$. The mathematics are analogous to the SJT model because both are bimolecular recombination models for entities with density proportional to $G/N_{\rm db}$. However, the H collision model provides an alternate derivation of $t^{1/3}$ creation kinetics free of the contradictions with experiment described above.

B. Transient solutions

We next consider the transient solutions of Eqs. (7) in the limit of $N_m \ll N_{\rm db}$ [Eq. (10)]. Equations (1) and (2) imply that mobile H and immobile DB's are normally created and annihilated in pairs. Therefore, the relative change of N_m is much greater than that of $N_{\rm db}$.

When illumination suddenly begins at $t=0$, Eq. (7a) can be solved for the rise of N_m:

$$N_m(t)=(k_{\rm H}N_{\rm H}G/k_{\rm db}N_{\rm db})[1-e^{-t/\tau_r}] + N_m(0)e^{-t/\tau_r} \tag{16a}$$

with

$$\tau_r=(k_{\rm db}N_{\rm db})^{-1}. \tag{16b}$$

Here I assume a near-constant $N_{\rm db}$ and ignore H collisions. The response time (τ_r) of N_m given by Eq. (16) is also the trapping time for mobile H to DB's [Eq. (2)].

Equation (16a) shows that when $N_m(0)$ is small, N_m grows toward the quasiequilibrium value given by Eq. (11). H collisions between mobile H lead eventually to an asymptotic $t^{-1/3}$ decay of N_m [Eq. (15)]. The competing processes produce an N_m maximum shown clearly by the numerical solutions of Sec. V B. The rise of N_m normally causes a latency time of at least τ_r for significant light-induced creation of metastable DB's.

If illumination is suddenly extinguished at $t=0$, N_m decays primarily through trapping at DB's [Eq. (2)]. The solution of Eq. (7a) is

$$N_m(t)=N_m(0)e^{-t/\tau_r}=N_m(0)e^{-k_{\rm db}N_{\rm db}t}, \tag{17}$$

where I again assume a near-constant value of $N_{\rm db}$ and ignore H collisions [Eq. (10) limit]. If the waiting time before measurement is less than a few τ_r, a decaying population of excess DB's that are not actually SW defects may be observed. These defects are simply DB's that have not yet been ''found'' by an excess photoexcited mobile H atom. Finally, the remnant N_m population can cause some creation of metastable SW DB's even after illumination is extinguished, a phenomenon that is important during pulsed laser illumination of *a*-Si:H (see Sec. IV F).

C. Light-induced annealing and saturation

Light-induced annealing is the photocarrier-induced emission of H atoms into transport from $M(\text{Si-H})_2$ and their recapture into DB defects according to the reverse process of Eq. (4). This process is insignificant compared to defect production during the early stages of light soaking. It becomes important when the $M(\text{Si-H})_2$ population rises to make the term $2k_{\rm HH}N_{\rm HH}G$ a significant fraction of the creation term, $k_cN_m^2$ in Eq. (8c). Saturation of the defect density occurs when all derivatives in Eqs. (8) are identically zero.

In this section, I derive closed-form solutions of Eqs. (8) in this steady-state, light-induced DB saturation limit. In the high-$N_{\rm HH}$ regime for which light-induced annealing is important, metastable DB's dominate the DB population because N_m and the initial DB density are both negligible. Therefore, $2N_{\rm HH} \approx N_{\rm db}$. Setting $dN_{\rm HH}/dt=0$ and substituting $N_{\rm db}/2$ for $N_{\rm HH}$ in Eq. (8c),

$$k_cN_m^2=k_{\rm HH}N_{\rm db}G. \tag{18}$$

TABLE I. Upper and lower bounds to model parameters, consistent with 65 °C experiments. Choice of one parameter limits the range of the other parameters (see text).

65 °C	k_H ($cm^3 s^{-1}$)	k_{db} ($cm^3 s^{-1}$)	τ_r (s)
Upper bound	10^{-27}	5×10^{-12}	10
Lower bound	5×10^{-30}	10^{-17}	2×10^{-5}

Setting $dN_{db}/dt=0$ in Eq. (8b), I again obtain Eq. (11) for N_m. Substituting Eqs. (11) and (13b) into Eq. (18), and solving for N_{db}, gives the steady-state or saturated DB density

$$N_{sat}=(GC_{sw}/2k_{HH})^{1/3}. \tag{19}$$

To calculate the saturation time t_{sat}, I assume that light-induced annealing remains unimportant during the approach to saturation. Then Eq. (14) implies $N_{sat}=N_{db}(t_{sat}) \approx (3C_{sw})^{1/3}G^{2/3}t_{sat}^{1/3}$, and substitution of Eq. (19) yields

$$t_{sat}=(6k_{HH}G)^{-1}. \tag{20}$$

The G dependences of Eqs. (19) and (20) were derived phenomenologically in Ref. 38. A weak dependence of N_{sat} upon G, consistent with Eq. (19), is observed.[38,39] The predicted dependence, $C_{sw}\propto N_{sat}^3$, is also observed.[40] The saturated mobile H density, N_m^{sat}, is obtained by substituting Eq. (19) into Eq. (11):

$$N_m^{sat}=\left(\frac{k_{HH}k_H N_H}{k_c k_{db}}\right)^{1/3} G^{2/3}. \tag{21}$$

The numerical simulations of Sec. V C exhibit the saturation behavior implicit in Eqs. (8) and outlined above.

D. Experimental bounds on model parameters

Both k_c and k_{db} are parameters describing diffusion of the mobile Si-H/DB and annihilation of a mobile DB with another DB [e.g., in Eq. (7)]. The sole difference is in the type of DB with which the annihilation occurs [Eqs. (2) or (3)], and this should matter little. Therefore, I assume that $k_c \approx k_{db}$, and Eq. (13b) becomes

$$C_{sw}=2k_H^2N_H^2/k_{db}. \tag{22}$$

Even with this simplification, considerable difficulty arises in estimating the parameters because broad ranges of C_{sw}, k_H, and k_{db} are consistent with the few experimental data available. Most SW data in the literature is taken between room temperature and $T=65$ °C, the temperature to which a strongly illuminated sample rises. The only available H emission data at temperatures below the SW annealing temperature are from light-induced D tracer diffusion experiments[30] at 65 and 135 °C. I summarize the experimental constraints in this section, and I calculate 65 °C upper and lower bounds to k_H, k_{db}, and τ_r. These bounds are listed in Table I.

Experimentally, $C_{sw}=10\ s\ cm^{-3}$ for a high-quality sample illuminated with about 1 sun at 20–30 °C and $C_{sw}=300\ s\ cm^{-3}$ for 3-W/cm^2 illumination at 50–70 °C.[41] I use $100>C_{sw}>10\ s\ cm^{-3}$ to estimate parameters of Table I because the lower illumination levels are relevant to most DB creation experiments. The H density, N_H, is taken to be about $5\times10^{21}\ cm^{-3}$.

Light-induced D tracer diffusion measurements establish rough limits of $2\times10^{-31}<k_H(135\,°C)<4\times10^{-28}\ cm^3$ and $k_H(65\,°C)<3\times10^{-28}\ cm^3$, under the assumption that H and D behave identically.[30] However, recent hot-electron degradation studies in c-Si transistors suggest that D emission is 10 to 50 times less efficient than the corresponding H emission.[42] Van de Walle and Jackson[43] propose that this results from comparatively inefficient coupling of the Si-H bending modes to the Si-Si lattice phonon modes, a hypothesis that is supported by recent infra red-absorption measurements in a-Si:H.[44] This poor coupling could enable the Si-H bond to store vibrational energy for emission better than the well-coupled Si-D bond.

Given this resistance of the Si-D bond to D emission, the estimate of k_H from D tracer experiments may be somewhat low. A better upper bound consistent with the D tracer measurements might be $k_H(65\,°C)<10^{-27}\ cm^3$. Measured early-time defect creation implies[30] (within the present model) that the H emission rate is greater than $5\times10^{-7}\ s^{-1}$ per H atom at $G=10^{23}\ cm^{-3}\ s^{-1}$ and 65 °C. This result gives a stricter lower bound and implies $10^{-27}>k_H(65\,°C)>5\times10^{-30}\ cm^3$.

Substitution of the bounds to k_H (65 °C) and C_{sw} into Eq. (22) gives $5\times10^{-12}>k_{db}(65\,°C)>10^{-17}\ cm^3\ s^{-1}$. Substitution of $N_{db}\approx10^{16}\ cm^{-3}$ into Eq. (16b) gives a range for the mobile H rise and fall times of $10s>\tau_r(65\,°C)>2\times10^{-5}$ s. Through Eqs. (16) and (17), this time governs the rise and fall of N_m. The metastable DB density appears to rise rather quickly during as little as 60 s of light soaking,[16,34] and the rate of creation has not been observed to depend upon the waiting time before DB measurement, consistent with this range for τ_r.

The mobile H diffusion coefficient D_m is proportional to the parameter k_{db} and can be estimated as follows. Mobile H hops between Si-Si bonds at a rate given by D_m/a^2, where a is the Si-Si bond distance of about 2.3×10^{-8} cm. Because a mobile H has a retrapping probability at each hop of N_{db}/N_{Si}, the retrapping rate per H is roughly $(D_m/a^2)(N_{db}/N_{Si})$. Here $N_{Si}\approx a^{-3}$ is the density of Si-Si bonds. Equating this retrapping rate to $k_{db}N_{db}$ [see Eq. 7(a)], $k_{db}\approx aD_m$. More rigorously,[45] one obtains

$$k_{db}=4\pi aD_m \tag{23}$$

for this diffusion-limited or Langevin capture process. The bounds on k_{db} in Table I imply $4\times10^{-11}>D_m(65\,°C)>10^{-5}\ cm^2\ s^{-1}$. Elsewhere, I will show this value is reasonable for H diffusion in a-Si:H and describe some implications.[46]

Isomura *et al.*[41] reported $C_{sw}=300\ s\ cm^{-3}$ for a high-quality sample light soaked at $G=3\times10^{22}\ cm^{-3}\ s^{-1}$ between 50 and 70 °C. The saturation DB density for that light soak was $N_{sat}\approx2\times10^{17}\ cm^{-3}$.[41] Substitution in Eq. (19) gives $k_{HH}\approx10^{-27}\ cm^3$, equal to the upper bound to k_H (65 °C) found in Table I. Because the reaction of Eq. (1) and the reverse reaction of Eq. (3) both involve emission of mobile

H from Si-H, one might expect $k_{HH} \approx k_H$. However, the higher energy of H in $M(\text{Si-H})_2$ may destabilize the H, giving $k_{HH} > k_H$.

Obviously, with such weak experimental constraints on the parameters, only qualitative conclusions can be drawn from any numerical work. To compute the numerical solutions of the model in Sec. V, I have used $k_H = 10^{-29}\,\text{cm}^3$, $k_{db} = k_c = 10^{-16}\,\text{cm}^3\,\text{s}^{-1}$, and $k_{HH} = 10^{-28}\,\text{cm}^3$.

E. Photocarrier-driven diffusion of mobile H

At low temperature or high illumination intensity, the diffusion of the mobile H must be driven by photocarriers, rather than by thermal excitation.[47] Carrier trapping at the mobile Si-H/DB complex is a likely candidate to drive this diffusion because the complex has a level within the energy gap. The electron (n) or hole (p) densities are normally given by $n,p \propto G^x$, where $0 < x < 1$. If D_m is proportional to carrier density, substitution of D_m in Eq. (23) yields

$$k_{db} \propto D_m \propto G^x. \tag{24}$$

In a previous paper,[9] I used the form of Eq. (24) for both k_{db} and k_c to show that the long-time creation kinetics are $N_{db}(t) \propto G^{2(1-x)/3} t^{1/3}$ when mobile H diffusion is carrier driven. The $t^{1/3}$-dependence of Eq. (14) is preserved because the branching ratio for H trapping between the reactions of Eqs. (2) and (3) is unaffected by the mechanism of mobile H diffusion. At 4.2 K, where thermal diffusion of mobile H is obviously negligible, Stradins and Fritzsche[34] obtained $t^{1/3}$ creation kinetics and a G dependence that implies[9] $x \approx 0.3$, a value compatible with the G dependence of n measured by light-induced ESR.[48] In contrast, the $t^{1/3}$ creation kinetics at 4.2 K are incompatible with the SJT derivation[23] of Eq. (14) because DB's do not participate significantly in carrier recombination.[9,34,35]

When the photogenerated carrier density is high, the Eq. (24) limit may also apply at room temperature and above. Because the $t^{1/3}$ creation kinetics do not depend upon the mechanism of mobile H diffusion, detailed studies of the G and T dependences of DB creation are required to determine conditions for the transition between thermal and carrier-driven H diffusion. In the following section, I develop approximate closed-form solutions for pulsed-laser illumination, high-intensity conditions for which it is reasonable to assume that mobile H diffusion is carrier driven.

F. Intense pulsed laser irradiation

1. Phenomenology and previous theory

Several groups have studied SW defect creation using intense pulsed-laser sources to accelerate DB production.[36,49,50] For 100-fs pulses repeating at 7 kHz, Stutzmann *et al.*[49] observed a rise of defect density $N_{db}(N_p) \propto N_p^{1/2}$ in undoped a-Si:H. Here N_p is the number of laser pulses and is proportional to the total illumination time. Tzanetakis *et al.*[36] irradiated undoped a-Si:H using intense 2-eV light from a dye laser with a pulse time of $t_p = 30$ ns and a repetition rate of 7–10 Hz, and observed

$$N_{db}(N_p) \propto G N_p^{1/2}. \tag{25}$$

This result confirmed the $N_p^{1/2}$ dependence of Ref. 49 for undoped a-Si:H.

In doped and compensated a-Si:H, however, Tzanetakis *et al.*[36] observed roughly

$$N_{db}(N_p) \propto G^{1/2} N_p^{1/4}, \tag{26}$$

instead of Eq. (25). Here the G dependence is derived from measurement at only two different intensities, and therefore the exponent of G is approximate. Given experimental uncertainty, the data could also be fit with the continuous-illumination $G^{2/3} N_p^{1/3}$ limit [Eq. (14)].

Stutzmann *et al.*[49] explained the $N_p^{1/2}$ dependence in undoped samples within the SJT hypothesis framework. They assume that most DB production is due to slowly decaying carrier densities that create defects by their recombination during the dark-time between pulses. However, the authors of Ref. 51 measured about 1-nsec decay time of carrier density between pulses, and found that creation between their 30-nsec pulses must be negligible if proportional to np. They[51] concluded that another explanation of Eq. (25) is needed. This section outlines an alternative approach based upon the H collision model of the SW effect.

2. H collision theory

The rise and decay times of N_m are given by τ_r, which depends upon whether the laser is on or off. Combining Eqs. (16b) and (23) yields

$$\tau_r = (4\pi a D_m N_{db})^{-1}, \tag{27}$$

where useful for clarity, I will notate τ_r by τ_r^d in the dark and by τ_r^p during the laser pulse. In the dark time between pulses, I assume that τ_r^d, D_m, and k_{db} are little changed from their low-light values estimated in Sec. IV D. During the pulse, I assume the high carrier densities increase D_m as in Eq. (24), and therefore $\tau_r^p \ll \tau_r^d$. However, direct τ_r^p, D_m, and k_{db} data are unavailable for the laser-irradiation carrier densities.

Table I then gives approximate limits of $10\,\text{s} > \tau_r^d(65\,^\circ\text{C}) > 2 \times 10^{-5}\,\text{s}$. Metastable defect creation by H collision will continue for times of order τ_r^d after illumination is extinguished, and long after the decay of photocarriers is complete. For the two experiments described in Sec. IV E[36,49] and yielding Eq. (25), the laser pulse times are 0.1 and 30 ns, laser-induced photocarriers decay in about 1 ns,[51] and the dark times between pulses, t_d, are 0.1 s and 0.1 ms. The duty cycle $t_p/(t_d + t_p)$ is tiny, from 10^{-8} to 10^{-6}, for these experiments. Most importantly, $\tau_r^d \gg t_p$. We must therefore consider the possibility that SW defect creation between pulses dominates over creation during the pulse.

In fact, the critical assumptions for modeling degradation are the relative magnitudes τ_r^p, τ_r^d, t_p, and t_d. There are then four easily calculated limits (A-D) for pulsed illumination of undoped films. Schematic diagrams of the time dependences of N_m during the first few laser cycles are shown in Figs. 4(a)–4(d), for the corresponding limits A–D. The diagrams of Fig. 4 are not drawn to scale, nor do they indicate any long-term effect upon N_m of SW defect creation. Limit A is defined by $\tau_r^p \gg t_p$ and $\tau_r^d \ll t_d$. Limit B is $\tau_r^p \ll t_p$ and $\tau_r^d \ll t_d$. Limit C is $\tau_r^p \gg t_p$ and $\tau_r^d \gg t_d$. Limit D is $\tau_r^p \ll t_p$ and $\tau_r^d \gg t_d$. In each limit, A–D, $\tau_r^d \gg t_p$, implying the

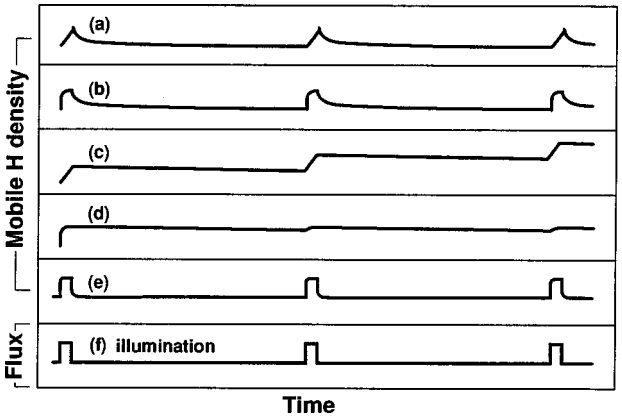

FIG. 4. Schematic time-dependence curves for the mobile H density during intense laser-pulse illumination. (a)–(e) correspond to limits A–E, respectively (see text). (f) indicates the incident laser intensity.

dominance of dark creation. For simplicity, boundary regimes between these limits are not treated here.

In doped or compensated films, no estimate of τ_r^d is available. Thus, a limit E for which $\tau_r^d \ll t_p$, must be considered. Of course, $\tau_r^p \ll t_p$ and $\tau_r^d \ll t_d$, also. The resulting time dependence of N_m is indicated schematically in Fig. 4(e). Only in this limit does creation during the laser pulse dominate over dark creation. The assumption that $\tau_r^d \ll t_p$ requires that τ_r^d be far smaller in compensated a-Si:H than in undoped a-Si:H. If so, this could be due to high densities of dopant traps for mobile H. In doped or compensated material, Eq. (27) would be replaced by

$$\tau_r = [4\pi a D_m (N_d + N_{\rm db})]^{-1}, \tag{28}$$

where N_d is the total dopant density.

In all limits, I assume that mobile H emission is given by $k_{\rm H} G N_{\rm H}$, as in Sec. III (see the discussion in the Appendix). Because $n,p \propto G^{1/2}$ during laser pulses,[51] this corresponds to emission proportional to the *np* product or electron-hole recombination rate. I ignore light-induced annealing. Theory is developed for all five limits in this subsection, and is compared to the experimental result in the following Sec. IV F 3.

Limit A ($\tau_r^p \gg t_p$ *and* $\tau_r^d \ll t_d$), *Fig. 4(a).* Mobile H does not build up over time, because N_m decays completely during t_d. Equation (16a) implies that $k_{\rm H} G N_{\rm H} t_p$ of mobile H are created during each pulse. Therefore, $N_m(0) = k_{\rm H} G N_{\rm H} t_p$ is the same at the end of each pulse and at the start of each dark decay. Here $t=0$ indicates the beginning of the N_m decay between pulses. Substitution in Eq. (17) gives the decay after each pulse,

$$N_m(t) = k_{\rm H} G N_{\rm H} t_p \, e^{-t/\tau_r^d}. \tag{29}$$

Substituting Eq. (29) into Eq. (12), and time integrating (at constant τ_r^d) yields $(k_{\rm H} G N_{\rm H} t_p)^2 k_c \tau_r^d$ new metastable defects per pulse. Although Eq. (29) may be incorrect in detail, the approximate scaling of defect creation with $G^2 \tau_r^d$ and the other quantities should be valid. Substituting $k_c \approx k_{\rm db}$ (see Sec. IV D) and τ_r given by Eq. (16b) for τ_r^d, the increase of $N_{db}(N_p)$ during the pulse numbered N_p is

$$\frac{dN_{\rm db}(N_p)}{dN_p} = \frac{(k_{\rm H} N_{\rm H} G t_p)^2}{N_{\rm db}(N_p)}. \tag{30}$$

Integration of Eq. (30) over N_p in the limit $N_{\rm db}(N_p) \geqslant 2N_{\rm db}(0)$ gives the long-time rise of N_{db},

$$N_{\rm db}(N_p) = \sqrt{2} k_{\rm H} N_{\rm H} t_p G N_p^{1/2}. \tag{31}$$

Limit B ($\tau_r^p \ll t_p$ and $\tau_r^d \ll t_d$), *Fig. 4(b).* Equation (16b) implies that the mobile H density saturates during each pulse. The quasiequilbrium mobile H population at the pulse end is then $N_m(0) = k_{\rm H} N_{\rm H} G / k_{\rm db}^p N_{\rm db}$ in analogy with Eq. (11). Here, the $k_{\rm db}$ value during the pulse, $k_{\rm db}^p(G)$, is likely given by Eq. (24). As in limit A, all mobile H is retrapped between laser pulses, so that N_m does not build up with time. The decay in the dark is

$$N_m = (k_{\rm H} N_{\rm H} G / k_{\rm db}^p N_{\rm db}) e^{-t/\tau_r^d} \tag{32}$$

by substitution of $N_m(0)$ into Eq. (17). Because most creation occurs during the time between pulses, the increase of $N_{\rm db}(N_p)$ with the pulse numbered N_p is obtained by substituting Eq. (32) into Eq. (12), and time integrating. Then

$$\frac{dN_{\rm db}(N_p)}{dN_p} = \frac{k_c (k_{\rm H} N_{\rm H} G)^2 \tau_r^d}{[k_{\rm db}^p N_{\rm db}(N_p)]^2} = \frac{(k_{\rm H} N_{\rm H} G)^2}{(k_{\rm db}^p)^2 [N_{\rm db}(N_p)]^3}, \tag{33}$$

where the rightmost form is obtained by substituting $k_c \approx k_{\rm db}$ in the dark and τ_r given by Eq. (16b) for τ_r^d. Integration of Eq. (33) over N_p gives the long-time rise of $N_{\rm db}$,

$$N_{\rm db}(N_p) = [2 k_{\rm H} N_{\rm H} / k_{\rm db}^p(G)]^{1/2} G^{1/2} N_p^{1/4}. \tag{34}$$

Tzanetakis, Kopidakis, and Fritzsche[51] found $n,p \propto G^{1/2}$ during their laser pulses, so $k_{\rm db}^p(G) \propto G^{1/2}$ would be the relevant form of Eq. (24) for mobile H diffusion driven by the electron or hole density. Substitution into Eq. (34) yields

$$N_{\rm db}(N_p) \propto (G N_p)^{1/4}. \tag{35}$$

Limit C ($\tau_r^p \gg t_p$ and $\tau_r^d \gg t_d$), *Fig. 4(c).* Mobile H is created during the laser pulse at a rate, $k_{\rm H} G N_{\rm H}$. In the dark, mobile H and DB's recombine according to Eq. (2) at a rate $k_{\rm db} N_m N_{\rm db}$, where $k_{\rm db}$ is the dark value. Figure 4(c) shows only the first few illumination pulses, and is therefore somewhat misleading. At long times, N_m actually rises to a quasiequilibrium value common to both the pulse and dark intervals; the cyclic variation in N_m is then small compared to N_m. A quasiequilibrium between N_m and $N_{\rm db}$ is reached when the creation and recombination of mobile H balance in each cycle

$$k_{\rm H} N_{\rm H} G t_p = k_{\rm db} N_m N_{\rm db} t_d, \tag{36a}$$

implying

$$N_m = k_{\rm H} N_{\rm H} G t_p / k_{\rm db} N_{\rm db} t_d. \tag{36b}$$

Equation (36b) is identical to Eq. (11), except that N_m is reduced by the factor t_p/t_d. This corresponds to an effective constant mobile H generation rate of $(t_p/t_d)G \ll G$. During the dark time between each pulse, N_m is nearly constant, as is the DB creation rate given by Eq. (12). Following the

mathematics of Sec. IV A, and substituting $t \approx t_d N_p$ because nearly all creation occurs in the dark, the long-time rise of $N_{\rm db}$ is

$$N_{\rm db}(t) = t_p^{2/3} t_d^{-1/3} (3C_{\rm sw})^{1/3} G^{2/3} N_p^{1/3}. \quad (37)$$

Here I have substituted $C_{\rm sw}$ from Eq. (13b).

Limit D ($\tau_r^p \ll t_p$ and $\tau_r^d \gg t_d$), Fig. 4(d). A quasiequilibrium mobile H population

$$N_m = k_{\rm H} N_{\rm H} G / k_{\rm db}^p N_{\rm db} \quad (38)$$

is reached during each laser pulse, in analogy with Eq. (11). This value depends upon $k_{\rm db}^p(G)$ during the pulse, again from Eq. (24). During the dark time between each pulse, N_m is nearly constant, as is the DB creation rate obtained by substituting Eq. (38) into Eq. (12). Following the mathematics of Sec. IV A, and substituting $t \approx t_d N_p$ because nearly all creation occurs in the dark, the long-time rise of $N_{\rm db}$ is

$$N_{\rm db}(t) = t_d^{1/3} [k_{\rm db} / k_{\rm db}^p(G)]^{2/3} (3C_{\rm sw})^{1/3} G^{2/3} N_p^{1/3}, \quad (39)$$

where $k_{\rm db}$ and C_{sw} take their dark values. Assuming (as in limit *B*) that $k_{\rm db}^p(G) \propto G^{1/2}$, and substituting into Eq. (39) yields

$$N_{\rm db}(N_p) \propto (t_d G N_p)^{1/3}. \quad (40)$$

Limit E ($\tau_r^d \ll t_p$, $\tau_r^d \ll t_d$ and $\tau_r^p \ll t_p$), Fig. 4(e). N_m rises so rapidly during the laser pulse it can be approximated by Eq. (38) during the entire pulse. N_m falls so rapidly in the dark that creation during the pulse dominates. The DB creation rate is given by substituting Eq. (38) into Eq. (12), with k_c replaced by its value during the pulse, k_c^p. Following the mathematics of Sec. IV A, the long-time rise of $N_{\rm db}$ is

$$N_{\rm db}(t) = t_p^{1/3} (3C_{\rm sw}^p)^{1/3} G^{2/3} N_p^{1/3}, \quad (41a)$$

with

$$C_{\rm sw}^p = \frac{2 k_c^p k_{\rm H}^2 N_{\rm H}^2}{(k_{\rm db}^p)^2}. \quad (41b)$$

Assuming $k_{\rm db}^p(G)$ and $k_c^p(G) \propto G^{1/2}$ from Eq. (24), and substituting into Eqs. (41), yields

$$N_{\rm db}(N_p) \propto G^{1/2} (t_p N_p)^{1/3}. \quad (42)$$

3. Experiment-theory comparison

For undoped *a*-Si:H, only the Eq. (31) result of Sec. II F 2 agrees well with the experimental result[36] given by Eq. (25). I conclude that the physically reasonable limit *A* is applicable to the laser-pulse creation of SW defects in undoped *a*-Si:H. In this limit, each laser pulse creates an identical density of mobile H, and all this mobile H decays completely during the dark time between pulses. SW defect creation occurs primarily in the dark. The experiments of Tzanetakis *et al.*[36] then imply that $\tau_r^p \gg 30$ ns and $\tau_r^d \ll 0.1$ s, consistent with the bounds on τ_r in Table I. The mathematics leading to Eq. (31) are similar to those used by Stutzmann *et al.* under that assumption of slow *photocarrier* decay and SW defect creation in the dark,[49] but the physics of the two derivations are completely different.

It is more difficult to identify the limit that obtains during laser-pulse illumination of doped and compensated *a*-Si:H.[36] Limits *B–E* are all reasonable candidates *a priori* because they have $N_{\rm db}(N_p) \propto N_p^{1/4}$ or $N_p^{1/3}$. More experimental study of the dependence of $N_{\rm db}(N_p)$ upon t_p and t_d could help settle the issue. It is not helpful that Eqs. (35), (40), and (42) all depend upon the assumption that $k_{\rm db}^p(G) \propto G^{1/2}$, which is reasonable but has no independent experimental support.

However, Eq. (37) of limit *C* and Eq. (42) of limit *E* appear to represent the best approximations to the data and to the approximate form[36] represented by Eq. (26). Assuming that limit *A* describes the undoped data, limit *C* would require that τ_r^d is much greater in doped than in undoped *a*-Si:H. This appears unlikely. Therefore, I speculate that Eq. (42) of limit *E* applies, with $G^{1/2} N_p^{1/3}$ kinetics governing the experiments on doped and compensated *a*-Si:H. Both τ_r^p and τ_r^d must then be much smaller in doped than in undoped *a*-Si:H, consistent with Eq. (28). The experiments of Tzanetakis *et al.*[36] would imply that $\tau_r^p \ll 30$ ns, shorter than Table I's 20-μs lower bound on τ_r in undoped films. In doped and compensated *a*-Si:H, N_m would saturate rapidly during the laser pulse, and would decay rapidly in the dark. SW DB creation would occur mainly during the laser pulse, in contrast to the case of undoped *a*-Si:H.

G. Compensation, doping, and electric-field-induced recovery

Compared with undoped *a*-Si:H, the light-induced DB creation rate is greatly decreased in compensated *a*-Si:H, but is increased in doped films.[52] Section IV F 3 above shows that Eq. (28) accounts for the laser-pulse creation kinetics in doped and compensated *a*-Si:H. Equation (28) implies that Eq. (11) for the quasiequilibrium between mobile H and defects is replaced by

$$N_m = (k_{\rm H} N_{\rm H} G) / [k_{\rm db} (N_d + N_{\rm db})] \quad (43)$$

in doped and compensated *a*-Si:H. Here N_d is the density of dopants that act as mobile H traps and reduce N_m. According to Eq. (12), the defect creation rate is proportional to N_m^2.

When dopants are added to amorphous silicon, there can be two competing effects upon N_m. First, there is an increase of $N_d + N_{\rm db}$ in the denominator that causes a reduction of the mobile H population, according to Eq. (43). Second, there can be a movement of the Fermi level away from midgap that reduces the formation energy of DB defects.

Skumanich, Amer, and Jackson[52] proposed that metastable DB formation is made easier by this shift of Fermi level. In the present model, the Fermi-level effect would be expected to increase the mobile H emission rate; that is, $k_{\rm H}$ will be greater in doped than undoped films. This increase of $k_{\rm H}$ causes an increase of N_m, according to Eq. (43). Of course, compensated films will exhibit no such increase of mobile H emission.

I propose that in compensated *a*-Si:H, an increase in $N_d + N_{\rm db}$ in the denominator of Eq. (43) reduces the mobile H population and therefore lowers the creation rate of SW DB's by H collision. However, in doped films, the increase of $k_{\rm H}$ in the numerator dominates over the $N_d + N_{\rm db}$ increase; both N_m and the defect creation rate increases.

Alternatively, the low-creation efficiency in compensated a-Si:H may be due to high internal electric fields which prevent formation of $M(\text{Si-H})_2$. Biswas and Pan[12] suggested that high electric fields would destabilize $M(\text{Si-H})_2$, because their proposed H_2* analog model of the complex has a large dipole moment.

These authors[12] pointed out that their proposal would also account for the high-electric-field annealing of SW DB's.[53,54] I add that electric-field induced destabilization of $M(\text{Si-H})_2$ may account for the quenching of the SW effect under high fields observed by Stradins and Fritzsche[4] at 4.2 K.

H. Irreversibility and molecular H formation

With minor modification, the H collision model accommodates the small irreversible component of light-induced defect creation that is observed. Irreversible defects are formed whenever photoexcited mobile H leaves a sample before retrapping at a DB according to Eq. (2). Carlson and Rajan[55] observed this effect in p-i-n devices illuminated under high reverse bias at elevated temperature. They found clear evidence that H had moved from the sample into the transparent conductive oxide contacts.[56]

A related source of irreversible DB creation would be formation of a H_2 molecule by collision of mobile H. The DB's left at the site of photoexcitation [Eq. (1)] become irreversible defects because of the strong H-H bond. Irreversible H_2 formation must be rare compared to metastable $M(\text{Si-H})_2$ creation, because H_2 formation requires simultaneous breaking of two Si-H bonds, while SW creation requires only the annihilation of two mobile DB's [Eq. (3)].

V. NUMERICAL SOLUTIONS

A. Algorithm, parameters, and initial conditions

Equations (7) and (9) and (8) and (9) are two sets of coupled differential equations for $N_m(t)$, $N_{\text{db}}(t)$, and $N_{\text{HH}}(t)$ under illumination and in the absence of thermal annealing. To study the H collision model, we have performed computer integration of these equations using the fourth-order Runge-Kutta algorithm with an adaptive time-step-size control.[57] Selected solutions were verified using a simpler iterative solution algorithm. Various parameter sets and initial conditions were investigated, and no convergence difficulties have been observed.

My emphasis here is placed on confirming the approximate closed-form solutions presented above and on exhibiting the qualitative behavior of the H collision model solutions. The qualitative features I describe are observed for a wide range of realistic initial conditions, light intensities, and parameters. More detailed comparison of the model with SW data will be presented elsewhere.[58]

In Section IV D, I describe the weak experimental constraints on the model parameters and generate the upper and lower bounds of Table I. Here, I show solutions for only a single parameter set: $k_{\text{H}}=10^{-29}\,\text{cm}^3$, $k_c=k_{\text{db}}=10^{-16}\,\text{cm}^3\,\text{s}^{-1}$, and $k_{\text{HH}}=10^{-28}\,\text{cm}^3$. The Si-H density is taken as $N_{\text{H}}=5\times10^{21}\,\text{cm}^{-3}$. Substitution in Eq. (13b) gives $C_{\text{sw}}=50\,\text{s}\,\text{cm}^{-3}$. Initial DB densities $N_{\text{db}}(0)$ vary from 10^{15} to $10^{16}\,\text{cm}^{-3}$ and substitution in Eq. (16b) gives τ_r near its Table I upper bound of 10 s. The initial mobile H concentration is $N_m(0)=0$ for the cases reported below. However, solutions were found to be extremely insensitive to the choice of $N_m(0)$ because N_m quickly equilibrates with N_{db}. The other initial condition, $N_{\text{HH}}(0)=N_{\text{db}}(0)/2$, corresponds to the assumption that equilibrium DB's form together with equilibrium $M(\text{Si-H})_2$ defects (see Sec. VI).

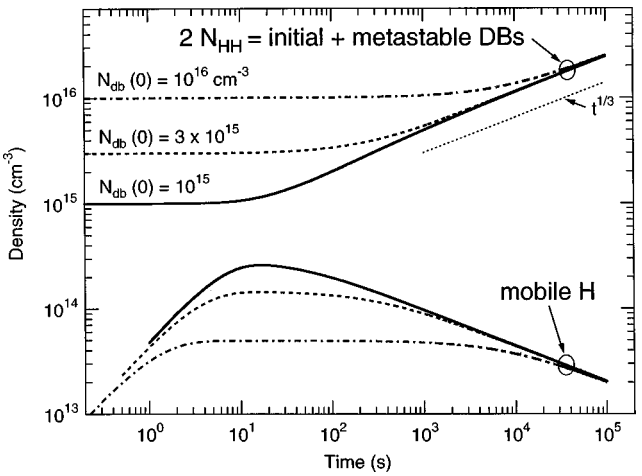

FIG. 5. Numerical solutions of Eqs. (7) and (9). $2N_{\text{HH}}(t)$ curves (upper) show the total density of DB's observed after illumination ceases. Corresponding $N_m(t)$ curves (lower) are indicated by their line type. Parameters are $k_{\text{db}}=k_c=10^{-16}\,\text{cm}^3\,\text{s}^{-1}$, $k_{\text{H}}=10^{-29}\,\text{cm}^3$, $N_{\text{H}}=5\times10^{21}\,\text{cm}^{-3}$, and $G=10^{21}\,\text{cm}^{-3}\,\text{s}^{-1}$. $N_{\text{db}}(0)=2N_{\text{HH}}(0)/2$ is indicated for each curve, and $N_m(0)=0$. The dotted line indicates the slope of a $N_{\text{db}}(t)\propto t^{1/3}$ line.

B. Creation at 1 sun

Figure 5 shows solutions of Eqs. (7) and (9) for a generation rate of $G=10^{21}\,\text{cm}^{-3}\,\text{s}^{-1}$, corresponding roughly to illumination with terrestrial solar irradiation (1 sun). $2N_{\text{HH}}(t)$ and $N_m(t)$ are presented for three different initial DB densities. In Fig. 5, the curves corresponding to the same initial conditions are indicated with the same line type. For example, the upper solid curve is $2N_{\text{HH}}(t)$, and the lower solid curve is $N_m(t)$, both for $N_{\text{db}}(0)=10^{15}\,\text{cm}^{-3}$. $2N_{\text{HH}}(t)$ corresponds to the sum of initial and SW metastable DB's in the sample. $2N_{\text{HH}}(t)$ is therefore the measured DB density in the sample after the incident light is extinguished at time t (assuming all the photoexcited mobile H's are retrapped to DB's). Figure 6 shows the actual DB density during illumination, $N_{\text{db}}(t)$, and also $2N_{\text{HH}}(t)$ for the $N_{\text{db}}(0)=10^{15}\,\text{cm}^{-3}$ solution of Fig. 5.

The solid $N_{\text{db}}(0)=10^{15}\,\text{cm}^{-3}$ curves of Fig. 5 exhibit the important qualitative features of the solutions. When the light is turned on, there is a rapid initial rise of N_m in accord with Eq. (16a). The duration of this rise is about 10 s, consistent with τ_r given by Eq. (16b). Because N_m approaches N_{db}, H collision retrapping soon competes with DB trapping and N_{HH} begins to rise. The increase in metastable DB's eventually reduces N_m. The asymptotic solution of $N_{\text{db}}(t)\propto t^{1/3}$ is approached at long times, as predicted by Eqs. (14) and (15). In general, N_m approaches N_{db} only for extremely high values of G or low values of $N_{\text{db}}(0)$, and then only briefly. Even in these cases, metastable defect creation soon restores $N_{\text{db}}\gg N_m$ [Eq. (10)].

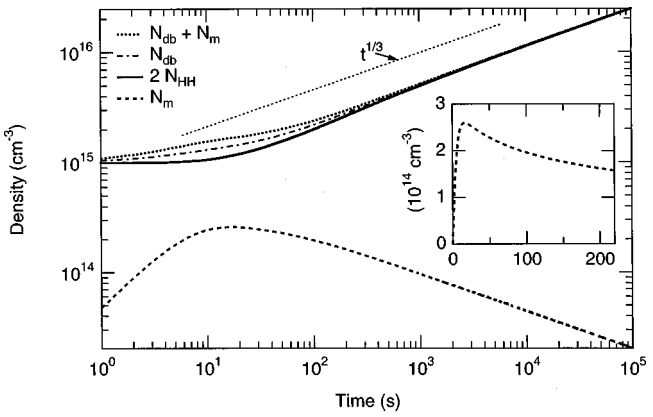

FIG. 6. Numerical solutions of Eqs. (7) and (9) for the parameter set of Fig. 5 and $N_{db}(0)=10^{15}\,cm^{-3}$. Quantities plotted are indicated in the legend, and discussed in detail in the text. The dotted line indicates the slope of a $N_{db}(t)\propto t^{1/3}$ line. Inset shows the same $N_m(t)$ data on linear scales with units of $10^{14}\,cm^{-3}\,s$.

Comparing the three solutions of Fig. 5, it is clear that low initial defect density results in a higher peak of N_m and therefore a more rapid onset of degradation. N_m begins to decay sooner as $N_{db}(0)$ is reduced. For the highest $N_{db}(0)=10^{16}\,cm^{-3}$, there is a 10^3-s period of approximately constant mobile H density, consistent with Eq. (16a). Because most mobile H's retrap at the copious DB's, some time is required for H collisions to raise $N_{HH}(t)$ and thereby reduce N_m. In Fig. 5, all curves converge after about 10 h of illumination; at long times, no memory of the initial defect density remains.

Figure 6 shows the solution for $N_{db}(t)$, the actual DB density in the sample during illumination, for the case of $N_{db}(0)=10^{15}\,cm^{-3}$. N_{db} is equal to $2N_{HH}$ at $t=0$, but immediately grows larger as mobile H is excited out of Si-H bonds. N_{db} remains larger than $2N_{HH}$ for nearly an hour—until metastable DB's dominate N_{db}. If the light is extinguished during this hour, mobile H will retrap rapidly at DB's and the DB density will fall after about τ_r to $2N_{HH}$; an insignificant number of mobile H's will collide to form metastable two-H complexes during the decay. In the long-time limit, metastable DB's dominate and $N_{db}=2N_{HH}$ once again.

The inset to Fig. 6 displays the same rise and fall of $N_m(t)$, but on linear scales. To observe $N_m(t)$ in the dark, the sample would have to be cooled in much less than τ_r after illumination ceases. Rapid cooling would prevent recombination of mobile H with DB's, and would freeze in $N_m(t)$. As discussed previously,[9] Darwich *et al.*[59] observed a rise and fall in infrared transmission spectroscopy lines upon light soaking and cooling which they attributed to mobile H. It is tempting to identify their observation with $N_m(t)$, but IR observation would require densities that are many orders of magnitude greater than $N_m(t)$ in Fig. 6.

Figure 6 also shows the sum $N_{db}+N_m$ during illumination. Because the mobile Si-H/DB complex likely contributes a gap state due to its mobile DB, this quantity may govern the measured defect density and the photocarrier density during the illumination. $N_{db}+N_m$ exceeds $2N_{HH}$ for nearly an hour, but in the long-time limit metastable DB's also dominate $N_{db}+N_m$. The mobile DB's may have different electronic or optical properties than ordinary DB's.

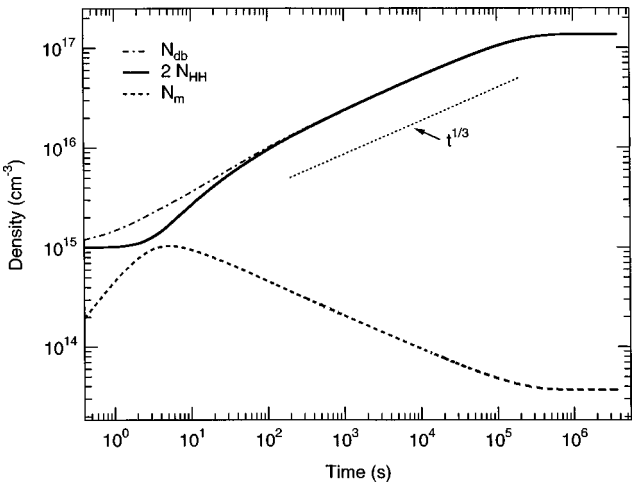

FIG. 7. Numerical solutions of Eqs. (8) and (9). Parameters are $k_{db}=k_c=10^{-16}\,cm^3\,s^{-1}$, $k_H=10^{-29}\,cm^3$, $k_{HH}=10^{-28}\,cm^3$, $N_H=5\times10^{21}\,cm^{-3}$, and $G=10^{22}\,cm^{-3}\,s^{-1}$. Initial conditions are $N_m(0)=0$ and $N_{db}(0)=10^{15}\,cm^{-3}$. The dotted line indicates the slope of a $N_{db}(t)\propto t^{1/3}$ line.

C. High-intensity illumination with saturation

Figure 7 shows solutions of Eqs. (8) and (9) for a generation rate of $G=10^{22}\,cm^{-3}\,s^{-1}$, corresponding roughly to 10 sun. $2N_{HH}(t)$, $N_{db}(t)$, and $N_m(t)$ are shown for $N_{db}(0)=10^{15}\,cm^{-3}$. Compared to 1-sum illumination (Fig. 6), there is a very rapid rise of N_m, until it is roughly $N_{db}/2$ for a few seconds after $t=2$ s. N_{db} increases together with N_m at the end of this rise, simply because DB's and mobile H's are created in pairs [Eq. (1)]. Only after about 2 s does the metastable DB density, $2N_{HH}$, begin to increase significantly. Both N_{db} and $2N_{HH}$ show roughly a $t^{1/3}$ rise before saturation at $N_{db}\approx1.4\times10^{17}\,cm^{-3}$, exactly the value predicted by Eq. (19). The saturation time is in good agreement with the value of 2×10^5 s predicted by the approximate equation (20).

VI. EQUILIBRIUM AND DARK EQUILIBRATION

A. Equilibrium

In the dark, H equilibrates between Si-H bonds and $M(\text{Si-H})_2$ complexes (the two deepest well bottoms in Fig. 1), unless slow kinetics prevents it. Above an equilibration temperature (T^*) at which H from Si-H bonds can transport freely between the configurations of Fig. 1, therefore, the DB density reaches its equilibrium value. The temperature dependence of N_{db} will be activated with $\Delta E=E_H-E_a$, the difference between the H diffusion activation energy and the onset energy for metastable DB annealing. The measured H diffusion energy is 1.4 to 1.5 eV,[11,60] and the DB annealing energy is about 1.1 eV.[16] Subtracting these measured quantities yields $\Delta E\approx0.3$–0.4 eV.

These consequences of Fig. 1 are consistent with experiment. Thermal equilibrium DB densities are observed[61] above an equilibration temperature, $T^*=200\,°C$.[62] Direct measurements of ΔE, by temperature-dependent *in situ* electron spin resonance, and by ESR after rapid quenching from elevated T, yield values of about 0.3 eV.[45,63]

Identifying of the Staebler-Wronski initial and final states as those governing defect equilibration explains a crucial ob-

servation about a-Si:H metastability: although ''native'' and light-induced DB's are indistinguishable experimentally, it is impossible to anneal away all DB's in a-Si:H. In the present model, there is no distinction made between native and light-induced defects. During light soaking, some pre-existing defects are annihilated by the reverse reaction of Eq. (4), but new DB's are formed at the same time. Some of the DB's created during a light soak will survive even after an anneal that removes excess SW defects. Each anneal of a sample restores the value of $N_{\rm db}$, but the DB's can be at different sites following each anneal.

This model of thermal equilibrium defect formation is a specific realization of the proposal of Street *et al.*[64] that a ''hydrogen glass'' mediates defect equilibrium reactions in a-Si:H. The present model also has parallels to the ''negative H correlation energy'' (negative U) model of Zafar and Schiff (ZS).[13] ZS proposed their model to explain both the rise of the DB density during H evolution and the thermal equilibrium DB density. However, ZS required that roughly half the H in a-Si:H is in negative-U pairs; they therefore identified the negative-U hydrogen with the clustered H phase observed by nuclear magnetic resonance.[65]

It may be possible to identify $M(\text{Si-H})_2$ with the clustered H of ZS and thereby unify the H collision and ZS models. However, the $M(\text{Si-H})_2$ center can only be identified with the copious clustered H sites ($N_{\rm HH}\approx N_{\rm H}/2$) if the vast majority of these sites are resistant to emission of mobile H by light. Otherwise, the last term on the right-hand side of Eq. (8a) is larger than the first term, and illumination produces mobile H without DB's. Photoexcited mobile H would then annihilate all the DB's by light-induced annealing, in contradiction to the experimental observation of SW DB creation by light.

B. Dark equilibration

If $N_{\rm db}$, N_m, and/or $N_{\rm HH}$ are not equal to their equilibrium value and the sample is above its equilibration temperature ($T>T^*$), the approach to equilibrium is governed by rate equations modified from Eqs. (8). In Sec. V B 1, I present appropriately modified equations. In Sec. V B 2, I discuss the thermal annealing of light-induced defects. In Sec. V B 3, I derive an expression for thermal creation of defects after rapid heating of a sample above T^*.

1. Rate equations

In the dark, light-induced mobile H emission is replaced by thermal emission. $R_{\rm H}$ is the rate per isolated Si-H of thermal H emission by the process of Eq. (2). $R_{\rm HH}$ is the rate of thermal H emission of the first H atom from $M(\text{Si-H})_2$. Emission of either H atom from $M(\text{Si-H})_2$ always creates two mobile H atoms by the reverse process of Eq. (3), as described in Sec. II A. The total emission rate of mobile H from $M(\text{Si-H})_2$ is $4R_{\rm HH}N_{\rm HH}$, and the annealing rate of $M(\text{Si-H})_2$ is $2R_{\rm HH}N_{\rm HH}$, by analogy with the discussion preceding Eq. (8). The rate equations in the dark are

$$dN_m/dt = R_{\rm H}N_{\rm H} - k_{\rm db}N_mN_{\rm db} - 2k_cN_m^2 + 4R_{\rm HH}N_{\rm HH}, \tag{44a}$$

$$dN_{\rm db}/dt = R_{\rm H}N_{\rm H} - k_{\rm db}N_mN_{\rm db}, \tag{44b}$$

and

$$dN_{\rm HH}/dt = -2R_{\rm HH}N_{\rm HH} + k_cN_m^2. \tag{44c}$$

Here, I have replaced all terms by which illumination generates mobile H in Eq. (8). When thermal creation, thermal annealing, light-induced creation, and light-induced annealing are all important, the rate equations must be further modified to include each unique term from both Eqs. (8) and (44).

2. Thermal annealing

Thermal annealing causes restoration of the equilibrium DB density after light soaking. In this subsection, I describe this process within the present model. During annealing, $N_{\rm HH}$ and $N_{\rm db}$ are well above their equilibrium values, and N_m is small. Normally, $4R_{\rm HH}N_{\rm HH}\gg R_{\rm H}N_{\rm H}$ and $k_{\rm db}N_mN_{\rm db}\gg R_{\rm H}N_{\rm H}$, so the thermal emission of mobile H from Si-H can be neglected in Eqs. (44). Then $2R_{\rm HH}N_{\rm HH}\gg k_cN_m^2$ also, and emission of mobile H from the right-hand well of Fig. 1 is crucial. Equation (44c) reduces to $dN_{\rm HH}dt=-2R_{\rm HH}N_{\rm HH}$, and the rate of thermal annealing is the simply the rate of H emission from $M(\text{Si-H})_2$. Every mobile H emitted from $M(\text{Si-H})_2$ is retrapped according to Eq. (2), and each one anneals a DB.

SJT[16] found that the thermal annealing energy E_a is normally 1.0–1.1 eV. However, after a 110 °C anneal, they reported that the annealing energy above 170 °C increases to more than 1.2 eV. SJT interpreted this increase as a partial annealing at 110 °C of a static population of metastable sites with a distribution of annealing energies.

Although a distribution of $M(\text{Si-H})_2$ sites could exist, I propose an alternative explanation of the observed increase in annealing energy. Each $M(\text{Si-H})_2$ site is formed by collision of two mobile H's. These H's bond to Si atoms in a locale that previously contained only satisfied Si-Si bonds. I postulate that the addition of two H atoms raises the local strain energy and accounts, in part, for the reduced H emission energy to transport (~1.1 eV) compared to emission from a normal Si-H bond (~1.5 eV). Local relaxation reduces this strain energy. Therefore, low-temperature annealing increases the thermal energy required to emit mobile H to transport and anneal SW DB's, as observed by SJT.[16]

During long or intense illumination, light-induced annealing means that $M(\text{Si-H})_2$ is repeatedly created and annealed. The least relaxed complexes are the most likely to be annealed, and a population of well-relaxed complexes will slowly build up. This accounts for the gradual increase of the thermal annealing energy of SW DB's with increasing illumination time.[62,66]

3. Thermal creation

Thermal creation of DBs is observed[61] upon heating (to $T>T^*$) a sample that was cooled slowly. In this subsection, I derive an expression for the kinetics of DB creation. After slow cooling, there is a low density of DB's, corresponding to equilibrium at T^*. Upon heating, $N_{\rm HH}$ and $N_{\rm db}$ are below their equilibrium value at T, so thermal creation dominates over thermal annealing. In this limit, $4R_{\rm HH}N_{\rm HH}\ll R_{\rm H}N_{\rm H}$ and $2R_{\rm HH}N_{\rm HH}\ll k_cN_m^2$ in Eqs. (44). The emission of mobile H from the right-hand well of Fig. 1 can be neglected. Equations (44) become

$$dN_m/dt = R_H N_H - k_{db} N_m N_{db} - 2k_c N_m^2, \quad (45a)$$

$$dN_{db}/dt = R_H N_H - k_{db} N_m N_{db}, \quad (45b)$$

and

$$dN_{HH}/dt = k_c N_m^2, \quad (45c)$$

identical to Eqs. (7), except that the rate of light-induced emission of mobile H ($k_H N_H G$) is replaced by its rate of thermal emission ($R_H N_H$). The solution of Eqs. (45), therefore, follows the solution described in Sec. IV A. After a time τ_r, quasiequilibrium in N_m is reached, and the DB density increases as

$$N_{db}(t) \propto t^{1/3}, \quad (46)$$

by analogy with the derivation leading to Eq. (14). I am not aware of experiments directly testing Eq. (46).

VII. CONCLUSIONS

This paper, and a previous short paper on the H collision model,[9] create a framework for understanding light-induced metastability in *a*-Si:H. Photocarrier recombination excites mobile H from Si-H bonds, leaving behind DB's. Mobile H ''collisions'' (associations) create metastable two-H complexes and metastable DB's. In contrast to most previous microscopic models of the SW effect, the H collision mechanism is consistent with ESR experiments and does not involve impurities.

Rate equations for the production of mobile H, DB's and $M(\text{Si-H})_2$ complexes are solved for quantitative predictions. The branching ratio between mobile H collisions and mobile H trapping to DB's yields $G^{2/3}t^{1/3}$ DB creation kinetics during continuous illumination. This branching ratio and the $t^{1/3}$ kinetics are unchanged down to 4.2 K, but at low temperatures the photocarriers must drive mobile H diffusion. The defect density increases as $Gt^{1/2}$ during intense laser-pulse illumination of undoped *a*-Si:H, because slowly decaying mobile H creates most SW DB's during the dark time between pulses. Earlier electron-hole pair recombination models of continuous and pulsed illumination kinetics lead to similar mathematical forms, but are inconsistent with other experimental results. The H collision model also describes thermal equilibrium and equilibration phenomena in *a*-Si:H.

ACKNOWLEDGMENTS

I thank Panos Tzanetakis, Hellmut Fritzsche, Dick Crandall, Stephan Heck, Rana Biswas, and Art Yelon for many helpful discussions and suggestions. S. Heck developed the Runge-Kutte program and assisted with the numerical work. P. Tzanetakis and the University of Crete Physics Department provided an excellent environment for physics during the early stages of work. The research was largely supported by the U.S. DOE under Contract No. DE-AC36-83CH10093. The Fulbright Foundation and the Foundation of Research and Technology Hellas in Greece supplied additional financial support.

APPENDIX

Equations (7)–(9) apply the zeroth-order approximation that illumination stimulates mobile H emission at the rate

$$R_m = k_H N_H G. \quad (A1)$$

Because the photocarrier recombination rate is equal to the generation rate, Eq. (A1) implies that every recombination event is equally likely to stimulate H emission. It is more likely, however, that only a subset of recombination events can supply the 1.4 to 1.5 eV required to excite mobile H from a Si-H bond. In this appendix, I describe alternatives to Eq. (A1) that may be better approximations to the physics of light-induced H emission, and derive the consequences for metastable DB creation.

Recombination through midgap DB levels supplies insufficient energy in any single step to stimulate H emission, and is therefore unlikely to be involved. Accurate modeling of the emission rate then requires a thorough understanding of photocarrier statistics, recombination processes, and the physics of recombination-induced H emission. Unfortunately, photocarrier physics in *a*-Si:H is complicated by a continuous density of gap states with a variety of capture rates.[67] There is a large, complicated, and often contradictory literature describing recombination and photoconductivity in *a*-Si:H.[68–72] It is unknown which of the various recombination processes (free-to-trapped, free-to-free, etc.) drive H emission, and what the precise dividing energy between free and trapped carriers may be at finite temperature.

To simplify the problem of estimating structural reconfiguration rates for a process requiring 1.4–1.5 eV, Stutzmann, Jackson, and Tsai[23] assumed that DB's mediate virtually all recombination in *a*-Si:H and thereby obtain free carrier densities, $n,p \propto G/N_{db}$. They then assumed the rate of structural reconfiguration is np. For H emission from Si-H, this approach implies

$$R_m \propto G^2/N_{db}^2. \quad (A2)$$

Equations (A1) and (A2) represent the extreme assumptions of no DB influence upon recombination and complete DB control of recombination, respectively. While R_m is most likely too complex for any simple form, Eqs. (A1) and (A2) can be generalized by taking the approximation $R_m \propto np$ of Ref. 23, but assuming more realistic forms for n and p. Then

$$R_m \propto G^\alpha/N_{db}^\beta$$

$$\text{with } 1<\alpha<2 \text{ and } 0<\beta<2, \quad (A3)$$

an expression that encompasses both Eqs. (A1) and (A2).

Modification of Eqs. (7)–(9) by Eq. (A3), and a detailed fitting of the metastability data is beyond the scope of this paper. However, long-time forms for $N_{db}(G,t)$ in the H collision model are easily obtained by assuming quasiequilibrium between the mobile H and DB populations, as in Sec. IV A. At quasiequilibrium, $N_m = R_m/N_{db}$ implies

$$N_m \propto G^\alpha/N_{db}^{\beta+1}. \quad (A4)$$

The rate of formation of metastable DB's by H collision (N_m^2) is then

$$dN_{db}/dt \propto G^{2\alpha}/N_{db}^{2(\beta+1)}. \quad \text{(A5)}$$

Integration of Eq. (A5) yields

$$N_{db} \propto G^{2\alpha/(2\beta+3)} t^{1/(2\beta+3)} \quad \text{(A6)}$$

at long times.

Equation (A6) corresponds to Eq. (14) for the Eq. (A1) approximation of $\alpha=1$ and $\beta=0$. In contrast, $N_{db} \propto G^{4/3} t^{1/7}$ is obtained by substitution of the exponents from Eq. (A2). This form is clearly at odds with experiment. Substituting the limits on α and β from Eq. (A3),

$$N_{db} \propto G^{\gamma} t^{\delta}$$

$$\text{with } \tfrac{2}{7} < \gamma < \tfrac{4}{3} \text{ and } \tfrac{1}{7} < \delta < \tfrac{1}{3}. \quad \text{(A7)}$$

Experimentally, a range of about $0.2 < \delta < 0.4$ is consistent with most data. The exponent γ is difficult to measure, but is roughly two thirds.[23] Because recombination physics depends upon G and N_{db}, measured exponents may depend upon the illumination level and could vary with time.

A future publication[58] will describe detailed fitting of $N_{db}(t)$ data to Eq. (8) as modified by forms similar to Eq. (A3). We find that exponents intermediate between those of Eqs. (A1) and (A2) yield good fits, even in the early-time regime where Eq. (13a) was shown to be inaccurate.[7]

[1] A. H. Mahan and M. Vanecek, in *Amorphous Silicon Materials and Solar Cells*, edited by B. L. Stafford, AIP Conf. Proc. No. 234 (AIP, New York, 1991), p. 195.

[2] D. Kwon, J. D. Cohen, B. P. Nelson, and E. Iwaniczko, in *Amorphous Silicon Technology—1995*, edited by M. Hack, E. A. Schiff, M. Madan, M. Powell, and A. Matsuda, MRS Symposia Proceedings No. 377 (Materials Research Society, Pittsburgh, 1995), p. 301.

[3] G. Ganguly, I. Sakata, H. Okushi, and A. Matsuda, Jpn. J. Appl. Phys., Part 2 **34**, L277 (1995).

[4] P. Stradins and H. Fritzsche, J. Non-Cryst. Solids **198-200**, 432 (1996).

[5] Y. Lee, L. Jiao, J. Hoh, H. Fujiwara, Z. Lu, R. W. Collins, and C. R. Wronski, in *Amorphous and Microcrystalline Silicon Technology—1997*, edited by E. A. Schiff, M. Hack, S. Wagner, R. Schropp, and I. Shimizu, MRS Symposia Proceedings No. 467 (Materials Research Society, Pittsburgh, 1997), p. 747.

[6] D. L. Staebler and C. R. Wronski, Appl. Phys. Lett. **31**, 292 (1977).

[7] H. Fritzsche, in *Amorphous and Microcrystalline Silicon Technology—1997* (Ref. 5), p. 19.

[8] M. Stutzmann, in *Amorphous and Microcrystalline Silicon Technology—1997* (Ref. 5), p. 37.

[9] H. M. Branz, Solid State Commun. **105/6**, 387 (1998).

[10] R. Biswas, Q. Li, B. C. Pan, and Y. Yoon, Phys. Rev. B **57**, 2253 (1998).

[11] H. M. Branz, S. E. Asher, and B. P. Nelson, Phys. Rev. B **47**, 7061 (1993).

[12] R. Biswas and B. C. Pan, Appl. Phys. Lett. **72**, 371 (1998).

[13] S. Zafar and E. A. Schiff, Phys. Rev. B **40**, 5235 (1989).

[14] K. J. Chang and D. J. Chadi, Phys. Rev. Lett. **62**, 937 (1989).

[15] S. B. Zhang, W. B. Jackson, and D. J. Chadi, Phys. Rev. Lett. **65**, 2575 (1990).

[16] M. Stutzmann, W. B. Jackson, and C. C. Tsai, Phys. Rev. B **32**, 23 (1985).

[17] H. M. Branz, R. S. Crandall, and M. Silver, in *Amorphous Silicon Materials and Solar Cells* (Ref. 1), p. 29.

[18] M. Stutzmann, in *Amorphous and Microcrystalline Semiconductor Devices, Vol. II: Materials and Device Physics*, edited by J. Kanicki (Artech House, Boston, 1992), p. 129.

[19] T. Kamei, N. Hata, A. Matsuda, T. Uchiyama, S. Amano, K. Tsukamoto, Y. Yoshioka, and T. Hirao, Appl. Phys. Lett. **68**, 2380 (1996).

[20] J. I. Pankove and J. E. Berkeyheiser, Appl. Phys. Lett. **37**, 705 (1980).

[21] M. Stutzmann, Philos. Mag. B **56**, 63 (1987).

[22] H. Dersch, J. Stuke, and J. Beichler, Appl. Phys. Lett. **38**, 456 (1981).

[23] M. Stutzmann, W. B. Jackson, and C. C. Tsai, Appl. Phys. Lett. **45**, 1075 (1984).

[24] S. Yamasaki and J. Isoya, J. Non-Cryst. Solids **164-166**, 169 (1993).

[25] D. L. Staebler and C. R. Wronski, J. Appl. Phys. **51**, 3262 (1980).

[26] D. Adler, J. Phys. (Paris) Colloq. **42**, C4-3 (1981).

[27] G. Schumm and G. H. Bauer, Phys. Rev. B **39**, 5311 (1989).

[28] R. Biswas, Q. Li, Y. Yoon, and H. M. Branz, Phys. Rev. B **56**, 9197 (1997).

[29] P. V. Santos, N. M. Johnson, and R. A. Street, Phys. Rev. Lett. **67**, 2686 (1991).

[30] H. M. Branz, S. Asher, H. Gleskova, and S. Wagner, following paper, Phys. Rev. B **59**, 5513 (1999).

[31] D. E. Carlson, Appl. Phys. A: Solids Surf. **41**, 305 (1986).

[32] W. B. Jackson and S. B. Zhang, in *Transport, Correlation and Structural Defects*, edited by H. Fritzsche, Advances in Disordered Semiconductors Vol. 3 (World Scientific, Singapore, 1990), p. 63.

[33] C. Godet and P. Roca i Cabarrocas, J. Appl. Phys. **80**, 97 (1996).

[34] P. Stradins and H. Fritzsche, Philos. Mag. B **69**, 121 (1994).

[35] For example, the decrease of 40-K electron-hole pair photoluminescence ($\sim$1.3 eV) at 40 K is not well correlated with increasing DB density [M. Yoshida and P. C. Taylor, in *Amorphous Silicon Technology—1992*, edited by A. Madan, M. J. Thompson, P. G. LeComber, Y. Hamakawa, and E. A. Schiff, MRS Symposia Proceedings No. 258 (Materials Research Society, Pittsburgh, 1992), p. 347.]

[36] P. Tzanetakis, N. Kopidakis, M. Androulidaki, C. Kalpouzos, P. Stradins, and H. Fritzsche, J. Non-Cryst. Solids **198-200**, 458 (1996).

[37] The constant k_c is lower by a factor of 2 than the conventional definition used for identical particle reactions in chemical kinetics.

[38] Z. Y. Wu, J. M. Siefert, and B. Equer, J. Non-Cryst. Solids **137&138**, 227 (1991).

[39] H. Gleskova, J. N. Bullock, and S. Wagner, J. Non-Cryst. Solids **164-166**, 183 (1993).

[40] M. Isomura and S. Wagner, in *Amorphous Silicon Technology—1992* (Ref. 35), p. 473.

[41] M. Isomura, H. R. Park, N. Hata, A. Maruyama, P. Roca i Cabarrocas, S. Wagner, J. R. Abelson, and F. Finger (unpublished).
[42] J. W. Lyding, K. Hess, and I. C. Kizilyalli, Appl. Phys. Lett. **68**, 2526 (1996).
[43] C. G. Van de Walle and W. B. Jackson, Appl. Phys. Lett. **69**, 2441 (1996).
[44] J.-H. Wei, M.-S. Sun, and S.-C. Lee, Appl. Phys. Lett. **71**, 1498 (1997).
[45] S. Zafar and E. A. Schiff, J. Non-Cryst. Solids **137**, 323 (1991).
[46] H. M. Branz (unpublished).
[47] P. Tzanetakis (private communication).
[48] R. A. Street and D. K. Biegelsen, Solid State Commun. **44**, 501 (1982).
[49] M. Stutzmann, J. Nunnenkamp, M. S. Brandt, A. Asano, and M. C. Rossi, J. Non-Cryst. Solids **137-138**, 231 (1991).
[50] R. Meaudre, S. Vignoli, M. Meaudre, and L. Chanel, Philos. Mag. Lett. **68**, 159 (1993).
[51] P. Tzanetakis, N. Kopidakis, and H. Fritzsche, J. Non-Cryst. Solids **198-200**, 276 (1996).
[52] A. Skumanich, N. M. Amer, and W. B. Jackson, Phys. Rev. B **31**, 2263 (1985).
[53] A. E. Delahoy and T. Tonon, in *Stability of Amorphous Silicon Materials and Devices*, edited by B. L. Stafford and E. Sabisky, AIP Conf. Proc. No. 157 (AIP, New York, 1987), p. 263.
[54] D. E. Carlson and K. Rajan, Appl. Phys. Lett. **70**, 2168 (1997).
[55] D. E. Carlson and K. Rajan, Appl. Phys. Lett. **68**, 28 (1996).
[56] D. E. Carlson and K. Rajan, Appl. Phys. Lett. **69**, 1447 (1996).
[57] W. H. Press, B. P. Flannery, S. A. Teukolsky, and W. T. Vetterling, *Numerical Recipes in Pascal* (Cambridge University Press, Cambridge, 1989).
[58] S. Heck and H. M. Branz (unpublished).
[59] R. Darwich, P. Roca i Cabarrocas, S. Vallon, R. Ossikovski, P. Morin, and K. Zellama, Philos. Mag. B **72**, 363 (1995).
[60] D. E. Carlson and C. W. Magee, Appl. Phys. Lett. **33**, 81 (1978).
[61] Z. E. Smith, S. Aljishi, D. Slobodin, V. Chu, S. Wagner, P. M. Lenahan, R. R. Arya, and M. S. Bennett, Phys. Rev. Lett. **57**, 2450 (1986).
[62] T. J. McMahon and R. Tsu, Appl. Phys. Lett. **51**, 412 (1987).
[63] R. A. Street and K. Winer, Phys. Rev. B **40**, 6236 (1989).
[64] R. A. Street, J. Kakalios, C. C. Tsai, and T. M. Hayes, Phys. Rev. B **35**, 1316 (1987).
[65] J. Baum, K. K. Gleason, A. Pines, A. N. Garroway, and J. A. Reimer, Phys. Rev. Lett. **56**, 1377 (1986).
[66] M. Kumeda, H. Yakomichi, A. Morimoto, and T. Shimizu, Jpn. J. Appl. Phys., Part 2 **25**, L654 (1986).
[67] J. G. Simmons and G. W. Taylor, Phys. Rev. B **4**, 502 (1971).
[68] R. H. Bube, Diffus. Defect Data, Part B **44-46**, 463 (1995).
[69] M. Q. Tran, Philos. Mag. B **72**, 35 (1995).
[70] K. Hattori, M. Anzai, H. Okamoto, and Y. Hamakawa, J. Appl. Phys. **77**, 2989 (1995).
[71] K. Lips, C. Lerner, and W. Fuhs, J. Non-Cryst. Solids **198-200**, 267 (1996).
[72] L. Jiao, S. Semoushikina, Y. Lee, and C. R. Wronski, in *Amorphous and Microcrystalline Silicon Technology—1997* (Ref. 5), p. 233.